https://doi.org/10.17221/111/2023-JFS

Sensitivity analysis and performance evaluation of neural networks for predicting forest stand volume – A case study: District 2, Kacha, Guilan province, Iran

Sima Lotfi Asl[1], Iraj Hassanzad Navroodi[2], Aman Mohammad Kalteh[3]*

[1]*Department of Forestry, University Campus, University of Guilan, Rasht, Iran*
[2]*Department of Forestry, Faculty of Natural Resources, University of Guilan, Sowmehsara, Iran*
[3]*Department of Rang and Watershed Management, Faculty of Natural Resources, University of Guilan, Sowmehsara, Iran*

**Corresponding author: s.lotfiasl@gmail.com*

Citation: Lotfi Asl S., Navroodi I.H., Kalteh A.M. (2024): Sensitivity analysis and performance evaluation of neural networks for predicting forest stand volume – A case study: District 2, Kacha, Guilan province, Iran. J. For. Sci., 70: 209–222.

Abstract: Tree volume is a characteristic used in many cases, such as determining fertility, habitat quality, growth size, allowable harvesting, and the principles of forest trade. It is imperative to develop methods that predict forest stand volume to obtain this extensive information quickly and cost-effectively. This study used supervised self-organising map (SSOM), multi-layer perceptron (MLP), and radial basis function (RBF) neural networks to predict forest stand volume based on physiography, topography, soil, and human factors. A sensitivity analysis method called the importance of prediction was used to determine how input variables influenced network output. First, the map of homogeneous units was prepared with ArcMap (Version 10.3.1, 2015) by combining digital layers to measure the tree's volume per hectare. Then, separate tree species in different diameter classes were measured in a circular grid of 200 m × 150 m, 0.1 ha of coverage, 3.3% sampling intensity, and a diameter at breast height (*DBH*) greater than 7.5 cm using systematic sampling on a homogeneous unit map in a regular random method. The neural network modelling results showed that SSOM, MLP, and RBF predicted forest stand volume most accurately according to physiography, topography, soil, and human factors. Furthermore, the sensitivity analysis results found that altitude above sea level, soil depth, and slope are the most influential input variables. In contrast, soil texture variables are the least effective at predicting forest stand volume.

Keywords: best matching unit; error back-propagation; importance of prediction neighbour function; spread; supervised learning

Forest habitats in the Hyrcanian or Caspian forests of Iran have different production capacities and a variety of trees and shrubs. This is due to the special geographical, climatic, and soil conditions (Mohammadi et al. 2010). Forest stand volume, one of the most critical characteristics of forest stands, is essential for planning and sustainable forest management. It determines fertility, habitat quality, growth size, allowable harvesting, and forest trade principles (Gebreslasie et al. 2010). It is imperative to develop methods that predict forest stand volume to obtain this extensive information quickly and cost-effectively (Bončina, Čavlović 2009). Artificial Neural Networks (ANNs) as a problem-solving, decision-making, and planning method in natural resource and forest management was first

https://doi.org/10.17221/111/2023-JFS

proposed by Coulson et al. (1987). ANNs (a subset of artificial intelligence) are a mathematical system with nonlinear learning and with parallel distributed processors called neurons (Haykin 1999). They help solve problems with large data sets that linear statistical methods cannot address (Liu et al. 2018). Learning is the main work of an artificial neural network, which involves adjusting neurons' weights and deviations. Keras, PyTorch, and TensorFlow stand as three influential deep-learning frameworks that have catalysed significant advancements in artificial intelligence. Each framework provides distinct features and advantages, rendering them suitable for diverse tasks and user preferences. Keras, functioning as a high-level neural networks application programming interface (API) scripted in Python, offers a user-friendly interface for constructing and training deep learning models. Renowned for its simplicity and accessibility, Keras serves as an optimal choice, particularly for novices, facilitating rapid prototyping without delving into intricate low-level programming intricacies. Conversely, PyTorch, a dynamic deep learning framework originating from Facebook's AI Research lab, prioritises flexibility and swiftness via its imperative programming paradigm. By enabling users to define computational graphs dynamically, PyTorch facilitates more efficient debugging and experimentation, thereby enhancing agility and adaptability in model development (Abadi et al. 2016; Dinghofer, Hartung 2020). There are two types of learning: unsupervised and supervised (Peng, Wen 1999). The feed-forward multi-layer perceptron (MLP) and radial basis function (RBF) are considered neural networks with supervised learning, whereas self-organising mappings (SOM) are considered neural networks with unsupervised learning (Stümer et al. 2010). Hu et al. (2020) studied forest volume prediction based on remote sensing and ground data using machine learning methods [such as Random Forest (RF), Support Vector Machine (SVM), and ANN] and kriging methods. Machine learning plays a crucial role in remote sensing, particularly in the analysis of satellite images. These algorithms possess the capability to automatically categorise various land cover types – ranging from forests, water bodies, and urban areas to agricultural land – within these images. They significantly aid in tasks such as identifying deforestation or shifts in land usage patterns, facilitating interventions and the formulation of effective policies (Chen, Zhang 2014; Belgiu, Drăguț 2016). Furthermore, these machine learning algorithms are instrumental in detecting alterations in sensing data by comparing images captured at different points in time. This capability enables precise measurement of landscape transformations, encompassing expansions, deforestation, or responses to natural disasters. Such precision proves essential in responding to emergencies, tracking trends in climate change, and strategically planning infrastructure initiatives (Pokhariyal et al. 2023). Lacerda et al. (2017) examined the performance of MLP neural networks and regression models in predicting tree volume in Brazilian savannas. Their findings showed that artificial neural networks and regression models efficiently predict tree volume. A study presented an overview of the SOM neural network as an unsupervised learning algorithm for water resources research by Kalteh et al. (2008). Klobucar and Subasic (2012) used the SOM neural network to analyse forest stand statistics. SOM neural network consists of neurons arranged in a hexagonal or rectangular structure in a one- or two-dimensional network. There are two layers to the SOM neural network: an input layer and an output layer (competitive layer or Kohonen), where all output layer neurons are connected to the weight vectors of the neurons in the input layer (Kalteh, Hjorth 2008). There is a more developed version of the SOM neural network called a supervised self-organising map (SSOM), which can predict data by applying specific changes and differs only in weight dimensions and estimation algorithms from the SOM neural network (Keller et al. 2018). SSOM neural networks have not been studied in forest sciences; therefore, this study aimed to investigate their capacities for predicting forest stand volumes using topographical, physiographic, soil, and human factors. The model was also compared to MLP and RBF neural networks for forecasting forest stand volumes. The sensitivity analysis method was then used to determine which variables significantly impact forest stand volume.

MATERIAL AND METHODS

Study area. District 2, Kacha, with a total area of 2 399 ha, is located in the Saravan forest, northern Iran (Figure 1). The study area is bounded by 49°32'24''E to 49°35'29''E on the east longitudes

https://doi.org/10.17221/111/2023-JFS

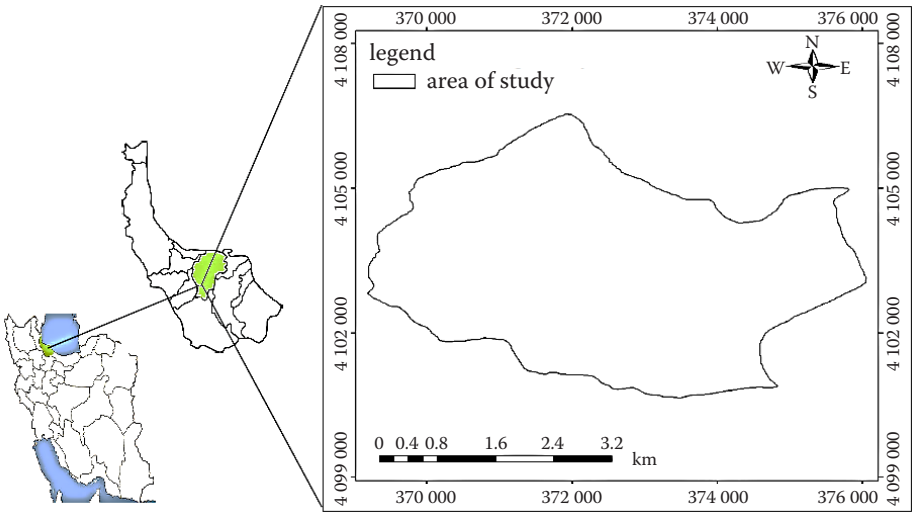

Figure 1. Geographical location of the District 2, Kacha, Guilan province, Iran

and 37°02'30"N and 37°05'42"N north latitudes. The elevation of the area is between 120 m a.s.l. and 785 m a.s.l. According to Dumarten's climate classification method, the average annual precipitation is about 1 255.7 mm, and the annual temperature of the research area is 16 °C. The climate of the study area is very humid. The study area is covered by broad-leaved tree species: *Fagus orientalis* Lipsky, *Carpinus betulus* L., *Diospyros lotus* L., *Alnus subcordata* C.A.M., and *Parrotia persica* (D.C.) C.A.M. District 2, Kacha forest management plan started in 1993, while local people previously used the forest mainly for fuel wood, construction, and human needs before.

Preparing homogeneous unit map. First, the map of homogeneous units was prepared with ArcMap (Version 10.3.1, 2015) by combining digital layers to measure the trees' volume per hectare. A digital elevation layer above sea level was created based on topographic maps with a scale of 1 : 25 000 and contour lines of 50 m. Then, it was classified into four height classes of 120–200 m, 200–400 m, 400–600 m, and 600–785 m, using the Reclassify tool. After that, the slope and aspect were obtained with the digital elevation layer. The aspect and slope map was classified with the Reclassify tool in terms of degree and percentage in four main directions and five layers: 0–25, 25–35, 35–45, 45–55, and 55–60, and the land unit map was obtained by overlaying them. Next, an environmental unit map-1 was created by combining the land unit map with the soil raster map in the geographic information system (GIS) environment. The regional soil type map is divided into four land sub-units based on essential soil characteristics such as bedrock, soil texture, and depth (Table 1). In the following step, the environmental unit map-2 was obtained by combining the environmental unit map-1 with the raster map of the distance from the road. All these steps were repeated to prepare a map of the distance from the stream. Eventually, the final environmental unit map with 124 homogeneous units was obtained (Natural Resources and Watershed Management Organization 2008).

Sampling of forest stand volume. Preliminary sampling was conducted randomly with 30 circular sample plots (n), covering 0.1 ha in the region.

Table 1. Soil type map classified following the United States Department of Agriculture (USDA) method

Codes	Composition of soil (%)			Classification	Soil depth (cm)	pH
	clay	silt	sand			
2-2-1	21–33	31–37	36–42	clay loam	50–55	6.8–7.2
2-1-2	25–35	33–40	22–42	clay loam	55–75	5.7–5.9
2-2-2	46–60	32–40	8–14	clay	75–90	7.3–7.4
3-2-3	28–49	21–38	28–34	clay	90–100	5.6–6.5

https://doi.org/10.17221/111/2023-JFS

This was done to determine the number of required sample plots. The following Equation (1) was then used to determine the number of sample plots (Zobeiry 2005; Table 2):

$$N = \frac{t^2 \times \mathrm{SD}\%^2}{E\%^2} \quad (1)$$

where:

N – number of sample plots required;
t – Student's t-test;
SD% – standard deviation percentage;
E% – percentage of statistical error.

In each sample plot, the diameter at breast height (*DBH*) species in different diameter classes was measured greater than 7.5 cm. Then, the forest stand volume was calculated based on the table of a single agent's local volume per hectare.

Forest stand volume modelling using artificial neural networks. Neural networks have emerged as fundamental components within the realm of artificial intelligence and machine learning. Notably, Radial Basis Function (RBF), Supervised Self-Organising Map (SSOM), and Multi-Layer Perceptron (MLP) networks stand out among the diverse neural network types, finding extensive applications across various domains. The activation function within a neuron serves as a pivotal element dictating its output, computed from the weighted sum of inputs. RBF networks commonly employ a Gaussian function as their activation function, enabling the network to model nonlinear relationships inherent in the data effectively. On the other hand, SSOM networks utilise a competitive activation function, activating the neuron with the closest weight vector to the input data. This mechanism enables SSOMs to autonomously organise and represent the topological relationships within the input data. Meanwhile, MLP neural networks, a form of feedforward neural network, employ multiple interconnected layers of nodes to process data. These networks use diverse activation functions, including sigmoid, tanh, ReLU, or softmax functions, enabling intricate data processing and feature extraction within various network layers. Distinguishing between RBF, SSOM, and MLP networks lies in their learning algorithms and diverse applications within neural networks. RBF networks specialise in function approximation and pattern classification, while SSOM networks demonstrate capabilities in both classification and regression tasks. Meanwhile, the multi-layer architecture and adaptable activation functions of MLP networks allow for their application across a broad spectrum of tasks, encompassing classification, regression, and time-series prediction. Despite their strengths, these neural network types share a unified objective: learning from data to formulate predictions or decisions. Their methodologies involve forward propagation where input data traverses the network to generate output and backward propagation, facilitating learning from errors and parameter adjustments to enhance performance. Selecting a suitable neural network depends on the nature of the problem at hand and the specific characteristics of the data. RBF neural networks prove effective for function approximation and pattern recognition, while MLP networks excel in addressing classification and regression challenges. SSOM neural networks, however, exhibit versatility, catering to both supervised and unsupervised learning tasks and accommodating labelled as well as unlabelled data sources (Kalteh, Hjorth 2008; Sharif Ahmadian 2015; Riese et al. 2020). In this study, the modelling of forest stand volume utilised SSOM, RBF, and MLP neural networks. The models were constructed based on input variables such as physiography (stream distance), topography (elevation, slope, aspect), soil properties (soil depth, silt, sand, clay, and pH), and human-related factors (road distance), with forest stand volume serving as the output variable (Figures 2–4).

The data must be normalised according to Equation (2) and placed between 0 and 1 to increase the

Table 2. Preliminary sampling with 30 random circular samples

$\overline{v}$	SD	SD%	E	E%	t	n	N
10.57	3.687	34.891	0.264	2.5	2	30	779

$\overline{v}$ – mean of characteristic of the study; SD – standard deviation, SD% – standard deviation percentage; E – standard error; E% – percentage of statistical error; t – Student's t-test; n – number of circular sample plots; N – number of sample plots required; the t-student table was also used to obtain t based on the number of sample plots and the probability level

https://doi.org/10.17221/111/2023-JFS

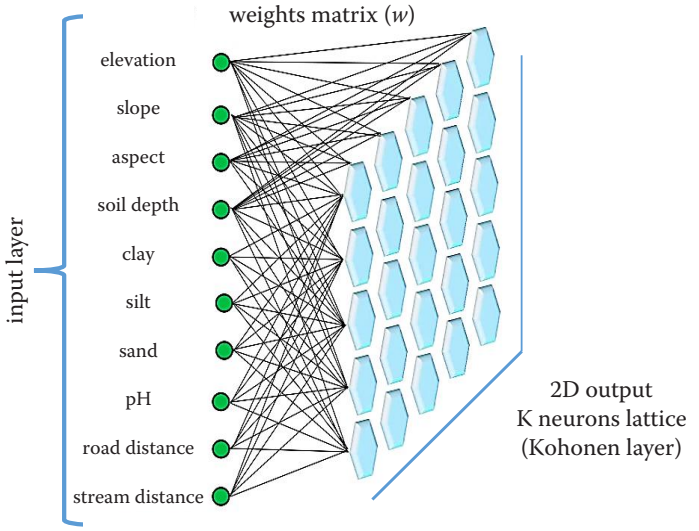

$$d_j = \left[\sum_{i=1}^{m}\left(x_i(t) - w_{ij}\right)^2\right]^{0.5} \qquad i = 1, ..., m;\ j = 1, ..., n$$

$$N_{j^*j}(t) = e^{-\frac{\left\|r_{j^*} - r_j\right\|^2}{2\delta^2_{(t)}}}$$

$$w_{ij}(t+1) = w_{ij}(t) + \eta(t) \times N_{j^*j}(t) \times [x_i(t) - w_{ij}(t)]$$

Figure 2. SOM (self-organising map) neural network with the structure (5 × 5; Kohonen 1982)

d_j – smallest distance from the input pattern; w_{ij} – weight value between input vector i and neuron j in the Kohonen layer; m – number of input variables; n – number of neurons in the Kohonen layer; $N_{j^*j}(t)$ – Gaussian neighbourhood function of winner neuron j^* in iteration t; δ^2 – radius of the neighbourhood in iteration t; $\left\|r_{j^*} - r_j\right\|$ – distance between the winner neuron and the neighbour neuron; $\eta(t)$ – learning rate in iteration t

speed and accuracy of neural network processes (Kalteh, Hjorth 2008):

$$Z = \frac{X_i - X_{\min}}{X_{\max} - X_{\min}} \tag{2}$$

where:

Z – normalised data;

X_i – used data;

$X_{\max}$, $X_{\min}$ – maximum and minimum values for each variable, respectively.

After data normalisation, 70% and 30% of them were assigned to the train data set (89 homogeneous units) and test data (35 homogeneous units), respectively (Keller et al. 2018). After data preprocessing, the best artificial neural network structure can be adjusted with parameters such as the number of neurons in the Kohonen layer, the number of input variables, and the evaluation criteria in the neural network. The test stage was determined by the coefficient of determination (R^2), adjusted R squared (R^2_{adj}), root mean squared error (*RMSE*),

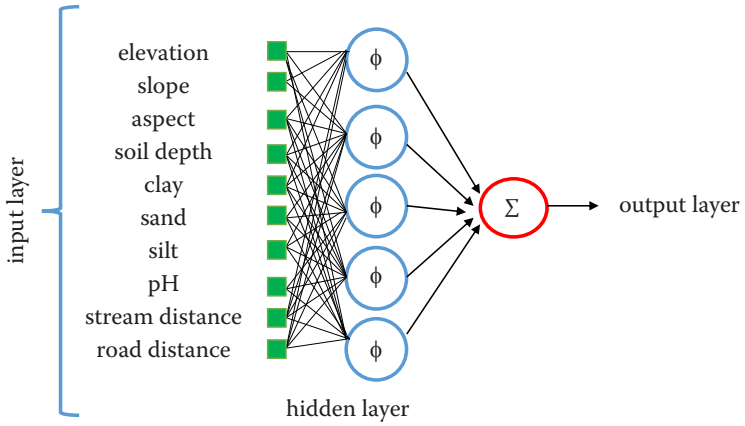

$$Y_j = \mathrm{f}\left\{\frac{\left\|X^p - U_j\right\|}{2\delta_j^2}\right\}$$

$$Z_{pk} = \sum_{j=1}^{l} Y_j W_{kj}$$

Figure 3. RBF (radial basis function) neural network with the structure (10-5-1; Fernando, Jayawardena 1998)

ϕ – Gaussian function; Y_j – response for the p^{th} input pattern X^p; $\left\|X^p - U_j\right\|$ – Euclidean norm; U_j – centre of the j^{th} radial basis function; δ – spread of the neural network containing that radial basis function; Z_{pk} – each node in the output layer produces a linear weighted sum of the hidden layer responses; W_{kj} – weight of the connection between neurons in the hidden and output layers

https://doi.org/10.17221/111/2023-JFS

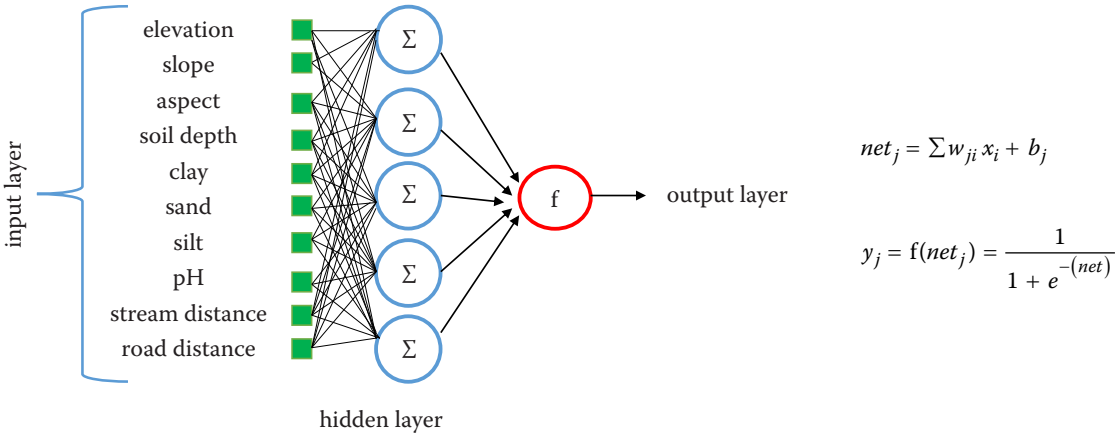

Figure 4. MLP (multi-layer perceptron) neural network with the structure (10-5-1; ASCE 2000)

Each neuron receives the weighted outputs of the neurons in the previous layer, the sum of these outputs forms the net input to neuron j (net_j); net_j – stimulus level of neuron j or net input to neuron j; w_{ji} – connection weight between nodes i; x_i – input to neuron i; b_j – bias of neuron j; y_j – Perceptron output

percent root mean squared error (*RMSE*%), mean absolute error (*MAE*), bias (*bias*) and percentage bias (*bias*%).

Sensitivity analysis. Sensitivity analysis is a tool used to understand how input variables affect a model's output. To conduct sensitivity analysis, it is essential to choose an appropriate procedure that accurately captures the interactions among variables. Reducing one input variable at a time is a common approach that simplifies the analysis and provides valuable insights into the individual effects of each variable. While this method may introduce additional complexity, it allows for a clearer understanding of how changes in each variable impact the output (Saltelli et al. 2004). Researchers utilise sensitivity analysis methods, such as predictive importance (*PI*), to gauge the degree of influence exerted by input data on network output. The prediction importance method involves systematically excluding an input variable and measuring the resultant change in root mean square error (*RMSE*) within the neural network. The observed increase in *RMSE* reflects the magnitude by which the network's error amplifies upon the removal of a specific variable. This change in error serves as a quantifiable indicator of the input variable's significance in shaping the network's output (De et al. 1997).

RESULTS

Descriptive statistics of the forest stand volume. As a result of analysing the volume of a single agent and calculating the volume of the forest stand by species per hectare, it was determined that the forest stand volume studied was 229.10 $m^3 \cdot ha^{-1}$, with *Fagus orientalis* Lipsky, *Carpinus betulus* L., and *Alnus subcordata* C.A.M. representing 43.36%, 23.26%, and 22.79%, respectively. Descriptive statistics of forest stand volume are shown in Table 3.

Figure 5 shows the average forest stand volume in homogeneous units. According to this figure, the average volume is between 200 silve·ha^{-1} and 300 silve·ha^{-1} in most units.

The statistics of mean, standard deviation, standard error, percentage of statistical error, and coefficient of variation were calculated for the forest stand

Table 3. Descriptive statistics of the forest stand volume

Characteristic	*Fagus orientalis*	*Carpinus betulus*	*Diospyros lotus*	*Parrotia persica*	*Alnus subcordata*	Other species	Total
Forest stand volume (silve·ha^{-1})	99.348	53.310	12.950	7.870	52.330	3.363	229.100
Frequency (%)	43.360	23.260	5.650	3.430	22.790	1.466	100.000

https://doi.org/10.17221/111/2023-JFS

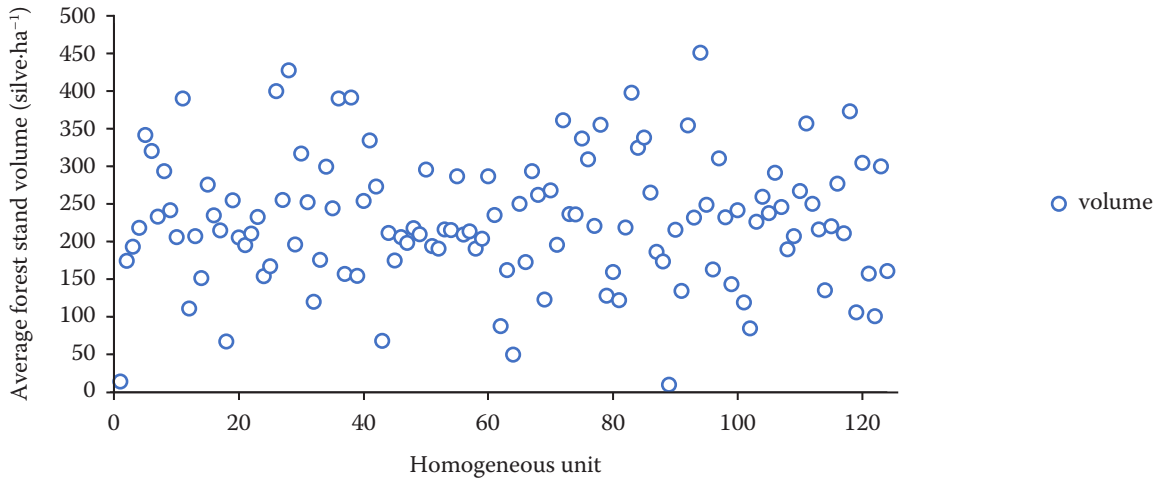

Figure 5. Average forest stand volume in homogeneous units

volume in the sampling. The results showed an average forest stand volume of 229.10 silve·ha^{-1} with a 4.28% statistical error. Table 4 indicates other statistics results.

Investigating the factors affecting forest stand volume. The correlation between physiographic, topographic, soil, and human variables with forest stand volume characteristics was analysed using Pearson's correlation coefficient. The results showed the highest correlation between the height above sea level and the slope and the volume of forest stands. This is so that forest stand volume increases with these factors increasing. It was, however, found that forest stand volume did not correlate significantly with slope direction and soil acidity. In contrast, soil factors such as soil texture (percentage of clay, silt, and sand) and soil depth significantly affect forest stand volume, and the intensity of correlation between them is at the lowest level. There is also an inverse relationship between forest stands and the distance from the stream and roads. Hence, the longer distance from roads (due to destructive effects) has better vegetation conditions (Wyman, Stein 2010). Table 5 displays Pearson's correlation coefficient results.

Table 4. The results of the forest stand volume inventory statistics (silve·ha^{-1})

Characteristic	$\overline{v}$	SD	E	E%
Forest stand volume (silve·ha^{-1})	229.10	13.70	0.49	4.28

$\overline{v}$ – mean of characteristic of the study; SD – standard deviation; E – standard error; E% – percentage of statistical error

Forecasting forest stand volume with artificial neural networks. A training of SSOM, RBF, and MLP neural networks was conducted using eight input variables (elevation above sea level, slope, soil depth, clay, silt, sand, and distance from road and the stream) and one output variable (forest stand volume) and then compared with their performance evaluation criteria (Table 6).

In the comparative evaluation of artificial neural networks during the test phase, it became evident that the (4 × 4) structured SSOM neural network outperformed both the RBF and MLP neural net-

Table 5. Pearson's correlation coefficient

Independent variables	Dependent variable
	forest stand volume (silve·ha^{-1})
Elevation (m)	0.684**
Slope (%)	0.672**
Aspect (°)	0.390^{NS}
Soil depth (m)	0.790**
Sand (%)	0.441**
Clay (%)	–0.551**
Silt (%)	0.167**
pH	0.780^{NS}
Stream distance (m)	–0.595**
Road distance (m)	0.576**

* Significance at 95% probability level; ** significance at 99% probability level; ^{NS} insignificance of correlation

https://doi.org/10.17221/111/2023-JFS

Table 6. The performance of SSOM, RBF, and MLP neural networks in predicting the volume of forest stand (silve·ha^{-1}) with eight input variables

Neural networks	Structure	Evaluation criteria							
		stages	R^2	R^2_{adj}	*MAE*	*RMSE*	*RMSE*%	*bias*	*bias*%
SSOM	4 × 4	training	0.9082	0.8788	11.38	27.85	4.85	11.38	3.89
		test	0.9541	0.9437	15.25	29.56	7.99	15.25	5.73
RBF	8-21-1	training	0.9164	0.8974	9.31	31.98	5.57	9.31	3.18
		test	0.9118	0.9890	18.94	32.67	8.83	18.94	7.13
MLP	8-15-1	training	0.8606	0.8332	12.56	40.87	7.10	12.56	3.43
		test	0.9137	0.9086	29.61	41.60	11.24	29.61	11.14

R^2 – coefficient of determination; R^2_{adj} – adjusted *R*-squared; *MAE* – mean absolute error; *RMSE* – root mean squared error; *RMSE*% – percentage of root mean squared error; *bias*% – percentage bias; 4 × 4 – number of Kohonen layer neurons in the SSOM neural network; 8-21-1 – number of neurons of input-hidden-output layers in the RBF neural network; 8-15-1 – number of neurons of input-hidden-output layers in the MLP neural network; SSOM – supervised self-organising map; RBF – radial basis function; MLP – multi-layer perceptron

works in terms of accuracy and error metrics. Remarkably, the SSOM network achieved an impressive R^2 value of 0.9541, indicating a robust correlation between predicted and actual values. Furthermore, it exhibited superior performance by showcasing a notably lower *RMSE* percentage (7.99%) and *bias* (15.25%) compared to its counterparts. Conversely, the RBF network, comprising 8 neurons in the input layer, 21 neurons in the hidden layer, and 1 neuron in the output layer, achieved an R^2 value of 0.9118. Its corresponding *RMSE*% was 8.83%, with a *bias* of 7.13%. Similarly, the MLP network, configured with 8 neurons in the input layer, 15 neurons in the hidden layer, and 1 neuron in the output layer, demonstrated an R^2 value of 0.9137, along with an *RMSE*% of 11.24% and a *bias* of 11.14%. The findings underscored the superiority of the SSOM neural network, specifically structured as (4 × 4), within this dataset or problem domain. Notably, employing a smaller network structure with fewer neurons exhibited higher accuracy and reduced error when contrasted against larger, more complex structures (Table 6).

The adaptation of observed and predicted forest stand volume values in SSOM, RBF, and MLP neural networks is shown in Figure 6. The SSOM neural network's observed and predicted values are primarily similar and slightly different, according to the above figure. However, there is a difference between the observed and predicted values in the MLP and RBF neural networks.

Predictive importance. *RMSE* values of neural networks were determined by comparing the error values for each model with their base errors (when all input variables are included) after removing one input variable (increase or decrease). Table 7 shows the status of the dropped variable. Table 8 also shows how artificial neural networks perform simultaneously with removing an input variable in two training and test stages.

Table 7 delineates the iterative process of eliminating input variables from a pool of eight factors [stream distance, road distance, elevation, slope, soil depth, clay (%), silt (%), and sand (%)]. Sequentially, in each step, one input variable is excluded, and the neural network is trained using the remaining variables. For instance, in Status 1, the road distance variable is omitted, and the neural network is then trained to utilise the remaining seven variables. This systematic procedure was iterated across all statuses, wherein each status designates the specific input variable omitted during training.

The analysis presented in Table 8 explores the consequences of removing individual input variables from the total input factors on the performance of SSOM, RBF, and MLP neural networks throughout both the training and test phases. The study findings underscore that the exclusion of an input variable from a neural network can elicit distinct effects on its performance across various scenarios. For instance, in Status 6 of the SSOM neural network, wherein the variable representing the

https://doi.org/10.17221/111/2023-JFS

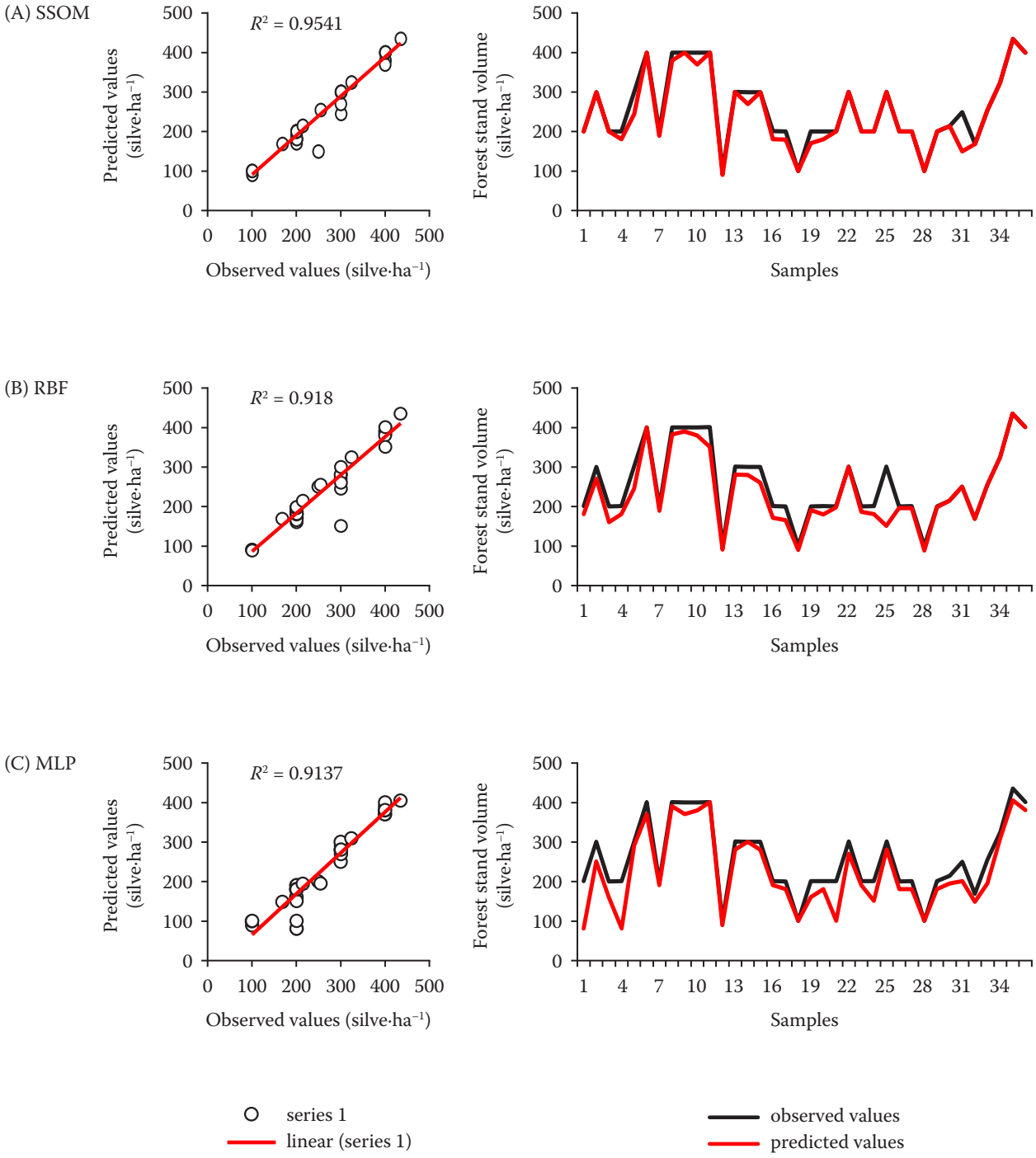

Figure 6. Comparison of the observed and predicted volume of forest stand (silve·ha^{-1}) with artificial neural networks: (A) Supervised self-organising map (SSOM); (B) radial basis function (RBF); (C) multi-layer perceptron (MLP)

Table 7. Status of dropped variable

	Status							
	1	2	3	4	5	6	7	8
Dropped variable	road distance	stream distance	elevation	slope	soil depth	clay (%)	silt (%)	sand (%)

https://doi.org/10.17221/111/2023-JFS

Table 8. The results related to the performance of neural networks while removing one variable from all the input variables

Status		Stages	R^2	R^2_{adj}	*MAE*	*RMSE*	*RMSE%*	*bias*	*bias%*
1	SSOM	training	99.46	99.37	2.04	11.63	2.02	2.04	0.70
		test	98.27	99.01	2.91	12.38	3.34	2.91	1.09
	RBF	training	98.40	96.60	4.57	18.41	3.20	4.57	1.56
		test	96.24	97.51	8.47	19.66	5.31	8.47	3.18
	MLP	training	95.40	94.69	5.30	23.00	4.00	5.30	1.81
		test	93.89	95.88	10.41	25.28	6.83	10.41	3.92
2	SSOM	training	98.26	97.94	3.85	14.31	2.49	3.85	1.31
		test	97.47	98.38	5.41	15.38	4.27	5.41	2.03
	RBF	training	96.35	95.70	5.21	20.69	2.46	5.21	1.78
		test	94.90	96.81	7.50	22.26	6.01	7.50	2.82
	MLP	training	94.43	93.26	7.62	25.92	3.08	7.62	2.61
		test	91.69	94.77	10.83	28.50	8.14	10.83	4.07
3	SSOM	training	94.05	92.66	8.46	27.05	3.22	8.46	2.89
		test	89.83	93.63	11.94	31.46	8.99	11.94	4.49
	RBF	training	90.61	88.33	10.15	34.11	4.06	10.15	3.47
		test	87.15	91.98	13.05	35.29	10.08	13.05	4.91
	MLP	training	86.51	83.93	11.72	40.03	4.76	13.53	4.63
		test	79.95	87.87	13.61	43.95	12.55	15.55	5.85
4	SSOM	training	91.90	90.25	8.59	31.17	3.17	8.59	2.94
		test	88.50	93.01	10.69	32.96	9.41	10.69	4.02
	RBF	training	90.57	88.82	10.15	33.38	3.97	10.15	3.47
		test	86.02	91.42	12.63	36.52	10.43	12.63	4.75
	MLP	training	84.93	82.34	11.96	41.97	4.99	11.96	4.09
		test	81.21	88.36	15.13	42.53	12.15	15.13	5.69
5	SSOM	training	92.25	94.25	6.98	23.94	2.85	6.98	2.39
		test	93.35	95.88	8.75	30.28	7.22	8.75	3.29
	RBF	training	90.63	89.31	10.84	32.64	3.88	10.84	3.71
		test	87.66	92.36	12.36	34.45	9.84	12.36	4.65
	MLP	training	86.82	87.60	12.40	35.16	4.18	12.04	4.12
		test	85.27	90.84	13.75	42.02	10.77	13.75	5.17
6	SSOM	training	99.37	99.27	1.80	8.48	1.00	1.80	0.61
		test	99.14	99.46	2.77	9.12	2.60	2.77	1.04
	RBF	training	98.79	98.67	2.65	11.47	1.36	2.65	0.90
		test	98.33	98.99	1.38	12.36	3.53	1.38	0.52
	MLP	training	98.59	98.43	2.89	12.49	1.48	2.89	0.98
		test	98.04	98.82	4.44	13.54	3.86	4.44	1.67

https://doi.org/10.17221/111/2023-JFS

Table 8. To be continued

Status		Stages	R^2	R^2_{adj}	*MAE*	*RMSE*	*RMSE*%	*bias*	*bias*%
7	SSOM	training	98.98	98.92	2.40	10.82	1.28	2.40	0.82
		test	98.65	99.17	3.88	11.09	3.22	3.88	1.46
	RBF	training	98.05	97.76	3.01	14.93	1.77	3.01	1.03
		test	97.67	98.53	5.55	15.09	4.31	5.55	2.09
	MLP	training	99.03	98.91	1.56	10.41	1.24	1.56	0.53
		test	98.45	98.01	4.72	12.36	3.53	4.72	1.77
8	SSOM	training	99.34	99.25	1.32	8.62	1.02	1.32	0.45
		test	99.09	99.06	3.77	12.01	3.43	3.77	1.40
	RBF	training	99.21	99.14	1.68	9.23	1.09	1.68	0.57
		test	98.07	98.02	3.33	10.27	2.93	3.33	1.25
	MLP	training	97.55	97.59	3.25	15.49	1.84	3.25	1.11
		test	97.00	98.17	5.55	16.83	4.80	5.55	2.09

R^2 – coefficient of determination; R^2_{adj} – adjusted *R*-squared; *MAE* – mean absolute error; *RMSE* – root mean squared error; *RMSE*% – percentage of root mean squared error; *bias*% – percentage bias; SSOM – supervised self-organising map; RBF – radial basis function; MLP – multi-layer perceptron

percentage of clay was eliminated, a noteworthy increase in both R^2 and adjusted R^2 values was observed during the test phase. Simultaneously, a decline in the *RMSE* and *bias* percentage was noted, indicating a marginal impact of removing the clay percentage variable on this particular neural network configuration. Contrarily, in Status 4 of the SSOM neural network, upon removal of the slope variable, a substantial decrease in both R^2 and adjusted R^2 values was evident compared to other scenarios. Additionally, there was a significant rise in *RMSE* and *bias* percentage during the test phase, signifying a considerable impact of excluding the slope variable on the performance of this specific neural network configuration. Similarly, in Status 8 of the RBF neural network, the exclusion of the sand percentage variable led to amplified R^2 and adjusted R^2 values, coupled with reduced root mean square error and *bias* percentage during the test phase when compared to alternative configurations. This observation implies a favourable impact of eliminating this specific input variable on the performance of this particular neural network mode. Conversely, Status 4 exhibited analogous trends in both SSOM and MLP neural networks, demonstrating a significant decline in both R^2 and adjusted R^2 values. This coincided with an escalation in *RMSE* and *bias* percentage during the test phase in comparison to alternative configurations. These findings underscore the pronounced effect of removing the slope variable on the performance of these particular neural network models. Overall, the order of artificial neural network error, from highest to lowest, is generalised as follows. Additional findings relevant to the performance metrics of artificial neural networks are detailed in Table 8.

SSOM 6 > SSOM 7 > SSOM 8 > SSOM 1 > SSOM 2 > SSOM 5 > SSOM 3 > SSOM 4

RBF 4 > RBF 3 > RBF 5 > RBF 2 > RBF 1 > RBF 7 > RBF 6 > RBF 8

MLP 6 > MLP 8 > MLP 7 > MLP 1 > MLP 2 > MLP 5 > MLP 4 > MLP 3

As compared to the base error, the neural network error of SSOM 4 (*RMSE* = 32.96; R^2 = 88.5), RBF 4 (*RMSE* = 36.52; R^2 = 86.02), and MLP 3 (*RMSE* = 43.95; R^2 = 79.95) increased by 3.4, 3.85, and 2.35, respectively. SSOM 6 (*RMSE* = 9.12; R^2 = 14.99), MLP 6 (*RMSE* = 13.54; R^2 = 98.04), and RBF 8 (*RMSE* = 10.27; R^2 = 98.87) neural network errors have also decreased by 20.44, 19.13, and 31.37, respectively (Figure 7).

https://doi.org/10.17221/111/2023-JFS

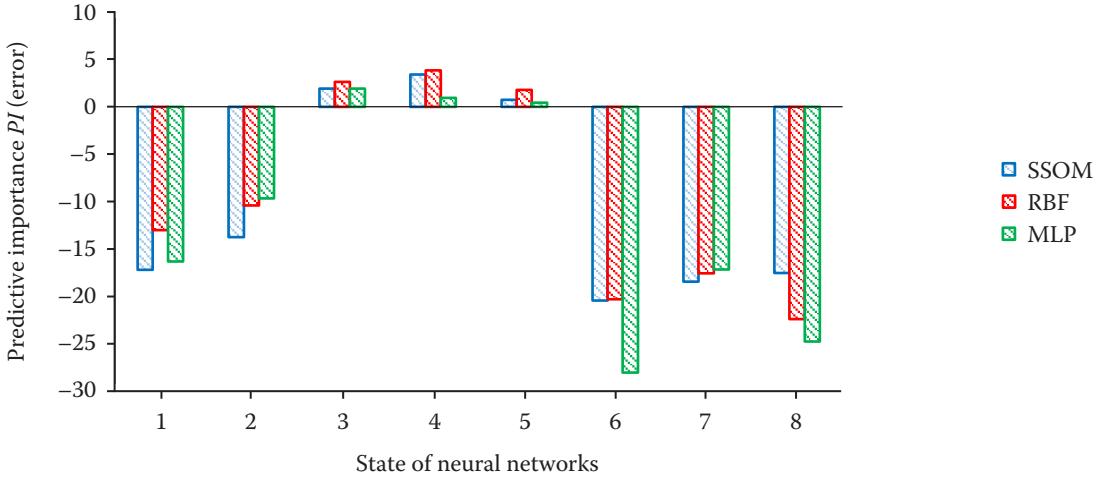

Figure 7. Sensitivity analysis

SSOM – supervised self-organising map; RBF – radial basis function; MLP – multi-layer perceptron

DISCUSSION

In natural ecosystems, frequent evaluations and timely information collection through field operations are complicated, exhausting, time-consuming, and expensive owing to the dynamic nature of the ecosystem (Kilpelanen, Tokola 1999). Forest managers are increasingly using low-cost methods (Naseri 2003). It has been demonstrated that artificial neural networks can be used to predict and estimate forest stand volume, as shown by Bayat et al. (2016), Özçelik et al. (2017), Ercanlı et al. (2018), Ronoud et al. (2019) and Bayat et al. (2020). Artificial neural networks, with their training, generalizability, and noise tolerance, can find hidden layers of dependent and independent variables with nonlinear, multivariate, and complex relationships (Ferraz Filho et al. 2018). Compared with evaluation criteria, this study used SSOM, MLP, and RBF neural network performance to predict forest stand volume by physiography, topography, soil, and human factors. The sensitivity analysis method was used to determine the effect of input variables on forest stand volume. While techniques like Principal Component Analysis (PCA) can provide dimensionality reduction, they may not be suitable for sensitivity analysis as they do not explicitly consider how changes in individual variables affect the output. Reducing one variable at a time can be a simpler and more effective approach for sensitivity analysis, providing valuable insights into individual effects without compromising accuracy or complexity. The choice of method depends on the specific goals and requirements of each analysis task (Saltelli et al. 2008). Pearson correlation coefficients were used to check whether the first input variables had a significant relationship before training the neural networks. The model was constructed using variables that had a significant relationship between them. Based on this study, the input variables significantly affect forest stand volume except for geography and soil acidity. Several studies have shown that environmental factors, such as height above sea level, slope, and geographical direction, play a substantial role in the development and formation of communities and vegetation, including Zhang et al. (2013) and Daghestani et al. (2017). The indirect effects of these factors affect trees' quantitative and qualitative characteristics, including their diameter at the breast, percentage of canopy cover, volume, and density of trees. As demonstrated by the results of Marvie Mohadjer (2006), Klippel et al. (2017), and Sefidi et al. (2018), forest stand volume is directly correlated with height above sea level. Hence, as height above sea level increases due to human interference and lack of access, the volume of tree stands increases, which confirms the present study's findings. Modelling was conducted in this study using variables such as height above sea level, slope, soil depth, percentage of clay, sand, and silt, and stream distance and road distance. According to the results, SSOM, RBF, and MLP neural networks predict forest stand volume based on the input variables. Based on the results of predictive importance, it was found that the neural networks SSOM 4 and RBF 4 by the slope variable and the

https://doi.org/10.17221/111/2023-JFS

neural network MLP 3 by the height above sea level variable had a greater impact. Also, the variable of clay percentage on the neural networks SSOM 6 and MLP 6 and sand percentage on the neural network RBF 8 had less effect. In this regard, Bayat et al. (2016) used the MLP neural network to estimate tree stand volume in the Grazin region. The results showed that the MLP neural network had the highest accuracy and lowest error than the regression model. Hu et al. (2020) used RF algorithms, SVM, and regression models to estimate forest reserves using Sentinel-2 satellite data. Their results indicated that the random forest algorithm had the highest performance among the other two models.

CONCLUSION

Based on the results of this study, the SSOM neural network performs better than the MLP and RBF neural networks when predicting forest stand volume by eliminating an input variable, as it has a low error rate and the highest adjusted coefficient of determination. Therefore, it can be selected as a suitable approach. According to Gil and Johnsson (2010), the SSOM neural network is similar to the RBF neural network in that it automatically determines how many RBFs need to be included in the hidden layer, and due to its increased accuracy and faster learning ability than the MLP neural network, it has a great deal of importance in resolving problems involving large data sets with a lot of features, which is supported by our findings. This statement highlights the potential significance of the research in guiding future studies on forest stand volume prediction in similar districts. By utilising the findings of this study, researchers can better understand the factors that impact forest stand volume and develop more accurate predictions for future forestry management.

REFERENCES

Abadi M., Barham P., Chen J., Chen Z.F., Davis A., Dean J., Devin M., Ghemawat S., Irving G., Isard M., Kudlur M., Levenberg J., Monga R., Moore S., Murray D.G., Steiner B., Tucker P., Vasudevan V., Warden P., Wicke M., Yu Y., Zheng X., Brain G. (2016): TensorFlow: A system for large-scale machine learning. 12th USENIX Conference on Operating Systems Design and Implementation, Savannah, Nov 2–4, 2016: 265–283.

Ahmadian A.S. (2015): Numerical modeling and simulation. In: Ahmadian A.S (ed.): Numerical Models for Submerged Breakwaters. Amsterdam, Elsevier: 109–126.

ASCE Task Committee on Application of Artificial Neural Networks in Hydrology (2000): Artificial neural networks in hydrology I: Preliminary concepts. Journal of Hydrologic Engineering, 5: 115–123.

Bayat M., Namiranian M., Omid M., Rashidi A., Babaei S. (2016): Applicability of artificial neural network for estimating the forest growing stock. Iranian Journal of Forest and Poplar Research, 24: 214–226. (in Persian)

Bayat M., Bettinger P., Heidari S., Henareh Khalyani A., Jourgholami M., Hamidi S.K. (2020): Estimation of tree heights in an uneven-aged, mixed forest in northern Iran using artificial intelligence and empirical models. Forests, 11: 324.

Belgiu M., Drăguț L. (2016): Random forest in remote sensing: A review of applications and future directions. ISPRS Journal of Photogrammetry and Remote Sensing, 114: 24–31.

Bončina A., Čavlović J. (2009): Perspectives of forest management planning: Slovenian and Croatian experience. Croatian Journal of Forest Engineering, 30: 77–87.

Chen J., Zhang M. (2014): Advances in machine learning applications in remote sensing. ISPRS Journal of Photogrammetry and Remote Sensing, 93: 1–2.

Coulson R.N., Folse L.J., Loh D.K. (1987): Artificial intelligence and natural resource management. Science, 237: 262–267.

Daghestani M., Zanganeh M., Taheri M. (2017): Investigation on quantitative characteristic and soil properties of *Juniperus excelsa* M. Bieb stands in Tarom Zanjan. Journal of Forest Research and Development, 3: 175–190. (in Persian)

De R.K., Pal N.R., Pal S.K. (1997): Feature analysis: Neural network and fuzzy set theoretic approaches. Pattern Recognition, 30: 1579–1590.

Dinghofer K., Hartung F. (2020): Analysis of criteria for the selection of machine learning frameworks. International Conference on Computing, Networking and Communications (ICNC), Big Island, Feb 17–20, 2020: 373–377.

Ercanlı I., Günlü A., Şenyurt M., Keleş S. (2018): Artificial neural network models predicting the leaf area index: A case study in pure even-aged Crimean pine forests from Turkey. Forest Ecosystems, 5: 1–12.

Fernando D.A.K., Jayawardena A.W. (1998): Runoff forecasting using RBF networks with OLS algorithm. Journal of Hydrologic Engineering, 3: 203–209.

Ferraz Filho A.C.; Mola-Yudego B.; Ribeiro A.; Scolforo J.R.S., Loos R.A., Scolforo H.F. (2018): Height-diameter models for *Eucalyptus* sp. plantations in Brazil. Cerne, 24: 9–17.

Gebreslasie M.T., Ahmed F.B., Van Aardt J.A.N. (2010): Predicting forest structural attributes using ancillary data and ASTER satellite data. International Journal of Applied Earth Observation and Geoinformation, 12: S23–S26.

https://doi.org/10.17221/111/2023-JFS

Gil D., Johnsson M. (2010): Supervised SOM based architecture versus Multilayer Perceptron and RBF networks. Expert Systems with Applications, 37: 4713–4718.

Haykin S. (1999): Neural Networks: A Comprehensive Foundation. Upper Saddle River, Prentice Hall: 842.

Hu Y., Xu X., Wu F., Sun Z., Xia H., Meng Q., Huang W., Zhou H., Gao J., Li W., Peng D., Xiao X. (2020): Estimating forest stock volume in Hunan province, China, by integrating *in situ* plot data, Sentinel-2 images, and linear and machine learning regression models. Remote Sensing, 12: 2–23.

Kalteh A.M., Hjorth P. (2008): Imputation of missing values in precipitation-runoff process database. Hydrology Research, 40: 420–432.

Kalteh A.M., Hjorth P., Berndtsson R. (2008): Review of the self-organizing map (SOM) approach in water resources: Analysis, modelling and application. Environmental Modelling and Software, 23: 835–845.

Keller S., Maier P.M., Riese F.M., Norra S., Holbach A., Börsig N., Wilhelms A., Moldaenke C., Zaake A., Hinz S. (2018): Hyperspectral data and machine learning for estimating CDOM, chlorophyll *a*, diatoms, green algae, and turbidity. International Journal of Environmental Research and Public Health, 15: 1–15.

Klippel L., Krusic P.J., Brandes R., Hartl-Meier C., Trouet V., Meko M., Esper J. (2017): High-elevation inter-site differences in Mount Smolikas tree-ring width data. Dendrochronologia, 44: 164–173.

Klobucar D., Subasic M. (2012): Using self-organizing map in the visualization and analysis of forest inventory. iForest – Biogeosciences and Forestry, 5: 216–223.

Kohonen T. (1982): Analysis of a simple self-organizing process. Biological Cybernetics, 44: 135–140.

Lacerda T.H.S., Cabacinha C.D., Araújo Júnior C.A.A., Maia R.D., Lacerda K.W.S. (2017): Artificial neural networks for estimating tree volume in the Brazilian savanna. Cerne, 23: 483–491.

Liu Z., Peng C., Work T., Candau J.N., Desrochers A., Kneeshaw D. (2018): Application of machine learning methods in forest ecology: Recent progress and future challenges. Environmental Reviews, 26: 339–350.

Marvie Mohadjer M.R. (2006): Silviculture. Tehran, University of Tehran: 387.

Mohammadi J., Joibary S.S., Yaghmaee F., Mahiny A.S. (2010): Modelling forest stand volume and tree density using Landsat ETM+ data. International Journal of Remote Sensing, 31: 2959–2975.

Natural Resources and Watershed Management Organization (2008): Revision Plan of District 2, Kacha, Guilan, Rasht. Tehran, Forestry Technical Office: 365.

Özçelik R., Diamantopoulou M.J., Brooks J.R. (2017): The use of tree crown variables in over-bark diameter and volume prediction models. iForest – Biogeosciences Forestry, 7: 132–139.

Peng C., Wen X. (1999): Recent application of artificial neural networks in forest resource management: An overview. In: Cortés U., Sànchez-Marrè M. (eds): Proceedings of the Meeting Environmental Decision Support Systems and Artificial Intelligence. Orlando, AAAI Press: 15–22.

Pokhariyal S., Patel N.R., Govind A. (2023): Machine learning-driven remote sensing applications for agriculture in India – A systematic review. Agronomy, 13: 1–30.

Riese F.M., Keller S., Hinz S. (2020): Supervised and semi-supervised self-organizing maps for regression and classification focusing on hyperspectral data. Remote Sensing, 12: 1–23.

Ronoud G., Darvish Sefat A.A., Fatehi P. (2019): Beech tree density estimation using Sentinel-2 data (Case study: Khyroud forest). SPRS International GeoSpatial Conference, Karaj, Oct 12–14, 2019: 891–895.

Saltelli A., Tarantola S., Campolongo F., Ratto M. (2004): Sensitivity Analysis in Practice: A Guide to Assessing Scientific Models. New York, Halsted Press: 466.

Saltelli A., Ratto M., Andres T., Campolongo F., Cariboni J., Gatelli D., Saisana M., Tarantola S. (2008): Global Sensitivity Analysis: The Primer. Chichester, Wiley Online Library: 291.

Sefidi K., Firouzi Y., Keivan Behju F., Sharari M., Rostamikia Y. (2018): Quantification of spatial structure of juniper stands in Kandaragh region. Iranian Journal of Forest, 10: 207–220. (in Persian)

Stümer W., Kenter B., Köhl M. (2010): Spatial interpolation of *in situ* data by self-organizing map algorithms (neural networks) for the assessment of carbon stocks in European forests. Forest Ecology and Management, 260: 287–293.

Wyman M.S., Stein T.V. (2010): Modeling social and land-use/land-cover change data to assess drivers of smallholder deforestation in Belize. Applied Geography, 30: 329–342.

Zhang Z.H., Hu G., Ni J. (2013): Effects of topographical and edaphic factors on the distribution of plant communities in two subtropical karst forests, southwestern China. Journal of Mountain Science, 10: 95–104.

Zobeiry M. (2005): Forest Inventory (Measurement of Tree and Stand). 3rd Ed. Tehran, University of Tehran Press: 308. (in Persian)

Received: October 14, 2023
Accepted: February 26, 2024
Published online: May 6, 2024